42. S. R. Su, M. O. O'Connor, and M. Levinson, *J. Mat. Res.*, **6**, 244 (1991).
43. A. F. Hepp, J. H. R. Gaier, W. H. Phillip, J. D. Warner, P. D. Hambourger, P. R. Aron, and J. J. Pouch, *Processing and Applications of High T_c Superconductors*, E. E. Mays, Editor, The Metallurgical Society (1988).
44. R. Ramesh, *Nature*, **346**, 420 (1990).
45. G. S. Grader, H. M. O'Bryan, and W. W. Rhodes, *Appl. Phys. Lett.*, **52**, 1831 (1988).
46. P. Reginier, L. Chaffron, X. Deschanels, and L. Schmirgeld.
47. J. E. Tkaczyk and K. W. Lay, *J. Mat. Res.*, **5**, 1368 (1990).
48. R. H. Arendt, A. R. Gaddipati, M. F. Garbauskas, E. L. Hall, H. R. Hart, Jr., K. W. Lay, J. D. Livingston, F. E. Luborsky, and L. L. Schilling, *Proc. Mat. Res. Symp.*, Materials Research Society, Pittsburgh, **99**, 203 (1988).
49. M. Murukami, M. Morita, and N. Koyama, *Jpn. J. of Appl. Phys.*, **28**, L1125 (1989).
50. S. Jin and J. E. Graebner, *Mat. Sci. Eng.*, **B7**, 243 (1991).
51. J. L. MacManus, in *Electrochemistry of Superconductors*, Report, Univ. of Cambridge, Cambridge (1988).
52. F. K. Lotgering, *J. Inorg. Nucl. Chem.*, **9**, 113 (1959).

Characterizations of Oxide Grown by N_2O

T. S. Chao, W. H. Chen, and S. C. Sun

National Nano Device Laboratory, Hsinchu 30050, Taiwan, China

H. Y. Chang

Institute of Electronics, National Chiao Tung University, Hsinchu, 300, Taiwan, China

ABSTRACT

The constitution of N_2O oxide has been investigated by using Auger analyses, ellipsometry measurement, and Fourier transform infrared (FTIR) spectroscopy in this paper. We found a nitrogen-rich layer formed at the interface of SiO_2/Si by Auger analyses. From the results of ellipsometry, we found the thinner the N_2O oxide, the larger the refractive index. A two-layer model construction of N_2O oxide was proposed for modeling the interfacial layer. We found that this layer thickness is 14 to 20 Å when the refractive index was set to 1.77. FTIR analyses show that some of the Si-O bonds were replaced by Si-N bonds. This is the reason that N_2O oxide has better electrical properties and a lower growth rate than those of the conventional dry O_2 oxide.

The growth of high quality gate oxide (<100 Å) film has become important for submicron devices of integrated circuits. Recently, there has been a growing interest in gate oxides grown or annealed in N_2O, instead of conventional dry O_2.[1,2] The oxide grown or annealed in N_2O ambient shows better electrical characteristics. A nitrogen-rich layer formed at the interface of SiO_2/Si has been reported in similarly annealed films. This layer is believed to reduce dangling Si and strained Si-O bond densities.[3] Hence, a more reliable device performance can be achieved.[4] However, very little information has been reported on the characterization of the N_2O oxide. In this paper, we first analyze the N_2O oxide by using Auger depth profiling analysis to characterize the interface properties. Ellipsometer has also been used to measure the refractive index of N_2O oxide grown at 950-1100°C. From the result of Auger and ellipsometery we propose a two-layer model of N_2O oxide constitution. We use multiple angle incident (MAI) ellipsometer method to confirm this interfacial layer. The bonding of N_2O oxide was studied by Fourier transform infrared spectroscopy (FTIR) in this work.

Experimental

p-Type, 4 in. silicon wafers (100) with resistivities of 15-25 Ω-cm were used as starting materials. After the standard RCA cleaning process and dipping with H_2O:HF (50:1), wafers were put into a furnace of the conventional resistive-heated type. High purity N_2O (>99.9995%) gas was used to grow oxide from 950-1100°C at increments of 50°C. The thickness of the oxides was measured by MAI ellipsometery to obtain an accurate refractive index and thickness. Some samples were also analyzed by Auger and FTIR spectroscopy.

Results and Discussion

Figure 1 shows the results of Auger depth profiling of N_2O oxide grown at 900°C for 30 min. Because the oxide was very thin, the energy of sputtering is 500 eV to obtain a higher concentration resolution. From the figure, it can be seen that a nitrogen-rich layer piles up at the interface of SiO_2/Si. The maximum concentration of N is about 4 ± 1%. This nitrogen-rich layer is different from that of nitridation of oxide in NH_3 ambient. In the case of the latter, nitrogen-rich layers were observed at both the interface and top surface of the oxide,[5] but were similar to the re-oxidization of NH_3 nitride oxide.[6]

The ellipsometer is a multiple-angle-incident-type with an incident wavelength at 632.8 nm. The incident angle is from 41.7 to 66.46° at increment of 0.24°. The total number of measured data of (Δ, ψ) is 104, where Δ and ψ are the ellipsometric angles. Δ is related to the degree of the polarizer angle, and ψ is related to the degree of the analyzer angle. To calculate the refractive index (N) and thickness (T) simultaneously, we used a one-layer model as shown in Fig. 3a. The refractive index of Si at 632.8 nm is assumed as 3.858-i0.018. There are two unknown parameters N and T in the system. In simulation processes, we changed the N and T to a reasonable range. T is from 0 to 500 Å, and N is from 1.460 to 1.500 Å, respectively. For assumed values of N and T, there exists a corresponding set (Δ_s, ψ_s) for incident angles,[7] where s means the simulated value. We calculated the sum of root-mean-square error between simulated value (Δ_s, ψ_s) and the measured (Δ_m, ψ_m) values for all incident angles. The equation is

$$\text{Error} = \left[\frac{1}{M}\sum_{i=1}^{M}\{(\Delta_s^i - \Delta_m^i)^2 + (\psi_s^i - \psi_m^i)^2\}\right]^{1/2} \quad [1]$$

usually, the error is dominated by the term of Δ.[8] The curve of error will reach a minimum as the best fitted value of N and T are found. The value of error in the simulation is about 0.341 to 0.399°. Figure 2 shows the results of the refractive index vs. thickness of different N_2O oxides grown at temperatures from 950 to 1100°C at increments of 50°C. It is seen that the refractive index of the films grown at 950, 1000, and 1050°C decreases as the thickness increases. The refractive index approached to 1.460 at thickness larger than 100 Å. For the N_2O oxide grown at 1100°C, the refractive index remains near 1.470 for all thicknesses. We believed that this is the case because more nitrogen atoms pile

Downloaded on 2014-04-28 to IP 140.113.38.11 address. Redistribution subject to ECS terms of use (see ecsdl.org/site/terms_use) unless CC License in place (see abstract).

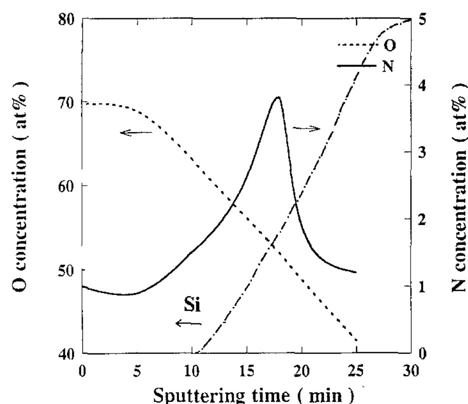

Fig. 1. The Auger depth profile of the concentration of O and N in the N_2O oxide grown at 900°C for 30 min (50 Å).

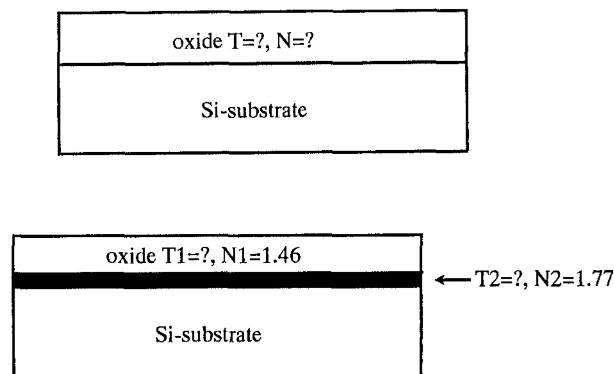

Fig. 3. (a, top) One-layer model of N_2O oxide by using multiple angle incident ellipsometer. (b, bottom) Two-layer model of N_2O oxide with an interface layer of N = 1.77 and thickness of T_2.

up at the interface resulting in an increasing refractive index. This increase of nitrogen concentration with an increase of growth temperature results in a negative influence of gate oxide quality. Yoon *et al.*[4] reported the time-dependent dielectric breakdown (TDDB) distribution and charge-to-breakdown Q_{BD} of N_2O oxide were severely degraded with increasing growth temperature from 950 to 1050°C while that of conventional oxide exhibits a slight improvement. They explained that this phenomenon was due to large undulations at SiO_2/Si interface observed by high resolution transmission electron microscopy (TEM). This undulation may be due to oversaturated nitrogen atoms at the interface. This phenomenon is consistent with the results of ellipsometry and would interfere with the ellipsometry measurement when undulation is high.

To understand more about the interfacial layer, we proposed a two-layer model in Fig. 3b. We assumed the interfacial layer is like a silicon oxynitride film with a composition near Si_2ON_2 (refractive index 1.77). This layer has been confirmed by ellipsometry and infrared spectroscopy by Naiman *et al.*[9] They found that this layer, formed at the interface of SiO_2/Si in high temperature ammonia nitridation, has a thickness 22 Å with a refractive index of 1.77. The unknown parameters in the system of Fig. 3b are T_1 of top oxide (N = 1.46), and T_2 of oxynitride film (N = 1.77). The calculation procedures are the same as Eq. 1 but with changed fitting parameters of T_1 and T_2. The value of T_1 is from 0 to 500 Å and that of T_2 is from 0 to 30 Å. The measured ellipsometric angles (Δ_m, ψ_m) are the same used for calculation of one-layer model. Table I shows the result for both the one- and two-layer model. The thickness of oxynitride (T_{oxy}) is around 17 ± 3 Å for the all different thicknesses and growth temperatures of N_2O oxide. The uncertainty maybe results from systematic errors. This thickness is close to the oxynitride film grown during the oxide nitrided by ammonia.[7] This implies that for N_2O oxidation there always exists an oxynitride film around 5-7 atomic layers at the interface of SiO_2/Si. This layer acts as a barrier for oxidizing species diffusing through the interface resulting in a slower growth rate.[3] The total thickness of this two-layer model is smaller than that of the one-layer model. The difference is 1-3 Å.

Figure 4 shows the reoxidation of N_2O. First, a sample (sample a) of N_2O oxide was grown in pure N_2O ambient at 900°C for 60 min. Another sample (sample b) of dry oxide as the control sample was grown in dilute O_2 (10%)/N_2 at the same temperature for 64 min. The thicknesses of samples a and b were 82 ± 2 Å and 79 ± 2 Å, respectively. We have controlled the growth rate of the two samples at the same level, about 1.3-1.4 Å/min. Then two samples were reoxidized in pure O_2 ambient for 15, 30, and 60 min. The change of thickness was shown in Fig. 4. It is obvious that the oxide grown initially in pure N_2O (sample a) grows more slowly than the oxide grown in conventional dry O_2 (sample b). This implies the interfacial layer of oxynitride does act as a barrier to the diffusing oxidizing species.

Figure 5 shows the result of measurements of FTIR. Sample a and the sample b with approximately the same thickness were evaluated for comparison. It was the same for sample c (reoxidized of sample a for 60 min in dry O_2, thickness is 195 ± 2 Å) and sample d (reoxidized of sample b for 30 min in dry O_2, thickness is 185 ± 2 Å). The peak wave number for sample a and b were almost the same at

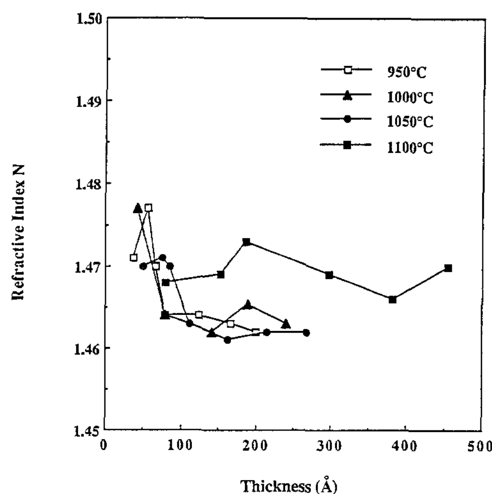

Fig. 2. The refractive index *vs.* thickness of N_2O oxide grown at 950, 1000, 1050, and 1100°C for 30 to 240 min.

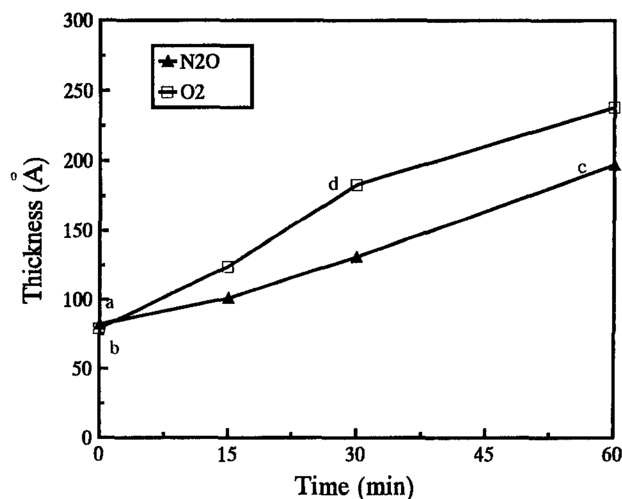

Fig. 4. Thickness of oxide grown in N_2O (sample a) and O_2 (10%)/N_2 (sample b) and reoxidized in pure O_2 at 900°C for 15, 30, and 60 min.

Downloaded on 2014-04-28 to IP 140.113.38.11 address. Redistribution subject to ECS terms of use (see ecsdl.org/site/terms_use) unless CC License in place (see abstract).

Table I. Refractive index, thickness, and RMS error of N_2O oxide using one- and two-layer models employing ellipsometry measurements.

	T_{ox} (A°)	N_{ox}	T_{ox} (N = 1.460)	T_{oxy} (N = 1.77)	T_{total} (Å)	RMS error
950 °C	37	1.471	15	19	34	0.341
	56	1.477	38	16	54	0.347
	67	1.470	44	20	64	0.359
	79	1.464	58	18	76	0.369
	125	1.464	103	19	122	0.358
	167	1.463	146	19	165	0.352
	201	1.462	182	17	199	0.361
1000°C	43	1.477	26	15	41	0.342
	65	1.467	49	14	63	0.375
	79	1.464	58	18	76	0.369
	141	1.462	121	17	138	0.382
	189	1.465	171	16	187	0.348
	240	1.463	224	14	238	0.351
1050°C	49	1.470	27	19	46	0.341
	75	1.471	55	17	72	0.353
	85	1.470	68	15	83	0.380
	111	1.463	90	18	108	0.360
	163	1.461	143	17	160	0.275
	214	1.462	193	18	211	0.359
	267	1.462	248	18	266	0.392
1100°C	79	1.468	56	20	76	0.360
	152	1.469	132	18	150	0.377
	187	1.472	168	18	186	0.379
	296	1.469	275	20	295	0.393
	381	1.466	361	18	379	0.366
	460	1.470	442	17	459	0.398

1100 cm^{-1} which results from the effect of absorbance of Si substrate.[10] Although with the same thickness, sample a has a lower peak intensity and a wider spectrum. This change in infrared spectrum indicates replacement of oxygen by nitrogen at the interface.[11,12] This replacement reduces the intensity of the main S-O peak. The IR spectrum of sample d shows the most intensive mode of oxide is due to Si-O anti symmetric stretch at 1070 cm^{-1}. Compared with sample b, sample d is thicker, hence it has a more intensive Si-O peak at 1070 cm^{-1}. Sample c has a lower peak Si-O intensity resulting from the replacement of O atom by N atom. Sample c also has a broadening of the antisymmetrical stretch and a shift of the peak wave number of 6 cm^{-1}. Koba *et al.*[12] have found the same phenomenon which is due to the partial replacement of doubly coordinated oxygen atoms by triply coordinated nitrogen atoms in the ammonia nitridation of SiO_2. From the comparison of the FTIRs, we concluded that N_2O oxide did have Si-N bonds formed at the interface of SiO_2/Si. This Si-N bond, instead of Si-O bonds of dry O_2 or Si-H bonds for NH_3 nitridation, is the reason for the low growth rate and the better electrical characteristic of N_2O oxide.

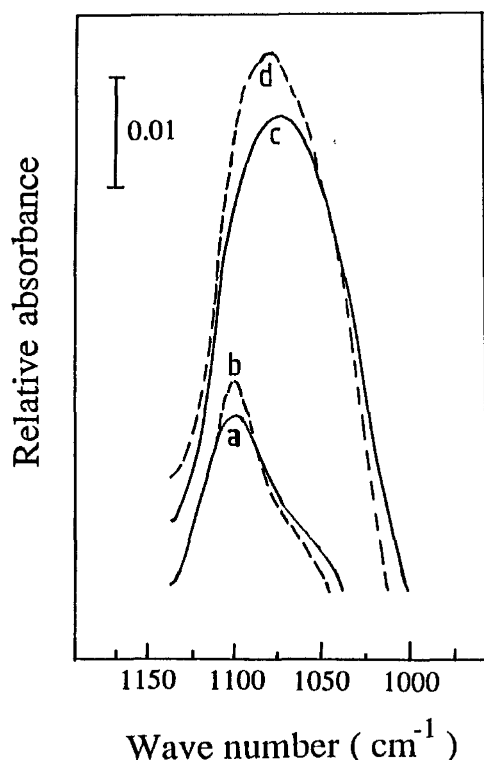

Fig. 5. FTIR spectrum of N_2O oxide and O_2 oxide. Sample a: N_2O oxide grown at 900°C for 60 min; b: O_2 (10%)/N_2 oxide grown at 900°C for 64 min; c: reoxidization of sample a in pure O_2 at 900°C for 60 min; d: reoxidization of sample b in pure O_2 at 900°C for 30 min.

Conclusions

In this work, the composition of N_2O oxide has been investigated by Auger analysis, multiple angle incident ellipsometry, and FTIR spectroscopy. From the Auger analyses, we found a nitrogen-rich layer at the interface of SiO_2/Si. The result of ellipsometry shows that thin N_2O oxide has a larger refractive index. We found that a two-layer model can be used to model the real constitution of N_2O oxide and the interface of SiO_2/Si. This interfacial layer can be modeled as an oxynitride film with a refractive index of 1.77 and a thickness of 14-20 Å. The result of FTIR indicated that some Si-O bonds at the interface of the conventional dry oxide were replaced by nitrogen as Si-N bonds in N_2O ambient. With a stronger bond energy than Si-O bonds, the interface of N_2O oxide has more stable and improved electrical properties than those of the conventional dry oxides.

Acknowledgments

This work is supported by the National Science Council of China through the contract No. NSC-83-0404-1009-190.

Manuscript submitted March 3, 1993; revised manuscript received June 3, 1993.

The National Science Council of China assisted in meeting the publication costs of this article.

REFERENCES

1. T. Y. Chu, W. T. Wong, J. Ahn, and D. L. Kwong, *This Journal,* **138,** L13 (1991).
2. H. Hwang, W. T. Ting, D. L. Kwong, and J. Lee, in *Proceedings of 22nd International Conference on Solid State Devices and Materials,* pp. 1155-1156 (1990).
3. W. Ting, H. Hwang, J. Lee, and D. L. Kwong, *J. Appl. Phys.,* **70,** 1072 (1991).
4. G. W. Yoon, A. B. Joshi, J. Kim, G. Q. Lo, and D. L. Kwong, *IEEE Electron Device Lett.,* **EDL-13,** 606 (1992).
5. F. H. P. M. Habraken, A. E. T. Kuiper, and Y. Tamminga,

Downloaded on 2014-04-28 to IP 140.113.38.11 address. Redistribution subject to ECS terms of use (see ecsdl.org/site/terms_use) unless CC License in place (see abstract).

J. Appl. Phys., 53, 6996 (1982).
6. T. Hori, H. Iwasaki, and K. Tsuji, *IEEE Trans. Electron Devices*, **ED-36**, 340 (1989).
7. S. S. So, *Surf. Sci.*, **56**, 97 (1976).
8. T. S. Chao, C. L. Lee, and T. F. Lei, *This Journal*, **138**, 1756 (1991).
9. M. L. Naiman, C. T. Kirk, B. L. Emerson, and J. B. Taitel, *J. Appl. Phys.*, **58**, 779 (1985).
10. F. Shimura, H. Tsuya, and T. Kawamura, *Appl. Phys. Lett.*, **37**, 483 (1980).
11. M. L. Naiman, C. T. Kirk, R. J. Aucoin, F. L. Terry, and P. W. Wyatt, *This Journal*, **131**, 637 (1984).
12. R. Koba, and R. E. Tressler, *This Journal*, **135**, 144 (1988).

Exploration of LOCOS-Type Isolation Limit Using SUPERSILO Isolation by Rapid Thermal Nitridation of Silicon

S. Deleonibus,* F. Martin, J. du Port de Pontcharra, and S. Tedesco

LETI (CEA-Technologies Advancées), Département de Microélectronique, Centre d'Etudes Nucléaires de Grenoble, 38041 Grenoble Cedex, France

ABSTRACT

The limits for overcoming shrinking localized oxidation of silicon type isolation in the subhalfmicron design rules area are considered: geometric limitations and field implant defect generation are investigated. A super sealed interface local oxidation (SUPERSILO) field isolation process using rapid thermal nitridation of silicon is characterized in terms of morphology, defect density, and electrical performance. With this isolation an encroachment lower than 100 nm is obtained in a large field area of 400 nm finished field oxide. Field oxide thinning and corner encroachment are minimized compared to other conventional isolations and make this process a better candidate for scaling down to 0.7 μm active area pitch design rules. The compatibility with low gate oxide defect density for a thickness as low as 7 nm is demonstrated. Several boron p^+ field channel stop implant processes are investigated by characterizing three different scenarios: implanting before field oxidation (classical), through field oxide after the oxidation mask removal (field-retro), and through the poly gate material (poly-retro). In order to avoid defect generation, the retrograde scenarios will be the solution in the future. The poly-retro scenario is the one that reduces boron segregation by a factor of about 10 with respect to the classical scenario and allows high performance without affecting the sustaining voltage. The use of a 0° tilt boron implant at 350 keV through the field oxide and poly gate material stack is shown to be practicable and reproducible.

Sealed interface local oxidation (SILO) field isolation has been widely described, and different sealing improvement methods have been tested during the past ten years.[1-3] Among them, rapid thermal nitridation (RTN) of silicon.[3,4] has received attention on account of its reproducibility. Despite its high performance, many problems arise in the use of this isolation scheme giving a bird's beak length of the order of 0.1 μm for a thick field oxidation.[5] The major issues are: (*i*) the sensitivity to gate oxide breakdown which is solved by the efficient removal of the sealing nitride (so-called nitride 1)[6] and (*ii*) optimization of layer thicknesses and field oxidation conditions to get a defect-free isolation.[3-5]

In this paper, we describe the optimization of SILO/RTN and SUPERSILO/RTN isolation schemes which are the simplest ways of fulfilling the requirements of deep subhalfmicron technologies by improving the field oxide thinning[7] achieving a near-zero bird's beak planarized field isolation while minimizing the heat cycle. We focus on the improvement of the major process steps (RTN, sacrificial oxidation,[8] etc.) which control oxide breakdown.

We also explain the impact of retrograde p^+ field channel stop implant that will avoid the defect generation limitation of the classical approach based on implanting before field oxidation on submicron design rules. Segregation of boron in the field oxide can thus be minimized by ultimately implanting boron through the stack of field oxide and poly gate before gate delineation. The body effect of metal oxide semiconductor N(MOS) transistors and shadowing effects are minimized by performing a 0° tilt implant, keeping a good performance of field isolation. Three doping scenarios are compared: (i) the classical scenario in which the field channel stop implant is performed before field oxidation, (*ii*) the field-retro scenario in which the field implant is performed through the field oxide after the field oxide growth and subsequent mask removal, and (*iii*) the poly-retro scenario in which the field implant is done through the poly gate material before gate delineation.

SILO/RTN and SUPERSILO/RTN schemes have been applied to 0.8 μm CMOS,[3-5] 16 Mbit erasable programmable read-only memory (EPROM),[3,9] and 0.35-0.50 μm high speed logic CMOS[10,11] by successfully scaling the isolation process. We show the scalability of this process for multimegabit generations design rules. Examples of applications and high voltage capabilities are given on 16-64 Mbit EPROM active and field devices.

Process Flow

The process sequence of SILO/RTN and SUPERSILO/RTN are described in Fig. 1. The field implant step has been omitted and will be discussed further in this section. In order to nitridize native oxide and achieve efficient sealing of nitride 1 on the silicon surface, RTN is performed after the wells definition in a rapid thermal processing (RTP) equipment in pure ammonia gas (NH_3) at atmospheric pressure between 850 and 1050°C.[5] The nitride 1 layer (10 nm) is deposited by low pressure chemical vapor deposition (LPCVD) at 715°C using SiH_2Cl_2 and NH_3. The buffer oxide layer (30 nm oxide 1) is realized at 690°C in an LPCVD reactor using a tetraethylorthosilicate (TEOS) source. Following the first oxide deposition a masking layer (50 nm nitride 2) is deposited. After patterning the active area, nitride 2 is etched in conventional reactive ion etching (RIE): oxide 1 and nitride 1 etching will require a high selectivity to silicon processing using a high pressure RIE reactor.[3,4] Polymer residues are eliminated by an O_2 RIE ashing followed by an HF dip (1.5% diluted in deionized water). A first-field oxidation is achieved at 950°C in a steam ambient following a 2 h drive-in under N_2 for activation and drive of the boron field implant if the field channel stop implant is performed first. Thus, oxygen is avoided

* Electrochemical Society Active Member.

Downloaded on 2014-04-28 to IP 140.113.38.11 address. Redistribution subject to ECS terms of use (see ecsdl.org/site/terms_use) unless CC License in place (see abstract).